Coastal Engineering 79 (2013) 32–41

Contents lists available at SciVerse ScienceDirect

Coastal Engineering

journal homepage: www.elsevier.com/locate/coastaleng

Wave parameters after smooth submerged breakwater

Dalibor Carevic *, Goran Loncar [1], Marko Prsic [2]

University of Zagreb, Faculty of Civil Engineering, Kaciceva 26, 10000 Zagreb, Croatia

ARTICLE INFO

Article history:
Received 30 September 2011
Received in revised form 6 April 2013
Accepted 8 April 2013
Available online xxxx

Keywords:
Smooth submerged breakwater
Wave period transformation
Zero crossing wave parameters
Spectral wave parameters
Smooth emerged breakwater

ABSTRACT

Based on the experimental studies of smooth submerged breakwater in the wave channel, it has been studied how the breakwater impacts on the changes of representative wave periods when the waves cross the breakwater. It has been shown that the reduction of the wave periods has a strong relationship with the wave steepness and relative submersion R_c/H_{m0-i}. Also, the impact of waves crossing the smooth submerged breakwater onto the Rayleigh's distribution of wave heights was investigated.

The influence of short and long waves generated after submerged smooth structure on temporal analysis has been investigated. The Lanczos filter was used for high and low frequency wave removal. It was concluded that long and short waves do not significantly influence the temporal analysis of periods.

The Van der Meer et al. (2000) model for the description of the transmitted spectrum has been improved so it gives better agreement with measurements. It was assumed that transfer of the energy from lower to higher frequencies vanishes linearly with a decrease in the relative submergence $-R_c/H_{m0}$. The energy transferred to higher frequencies is assumed as uniformly distributed between $1.5f_p$ and $3.2f_p$.

1. Introduction

It is usual in the calculation of run up, overtopping, morphological changes and reflection from perforated seawalls to use the characteristic heights and periods of incoming irregular waves. If any mentioned coastal structure is defended by smooth submerged structures, it is important to calculate the modified wave parameters after the submerged breakwater. Considering that low crested structures are mostly permeable (rubble mound), the results of this work cannot be used as general findings, but can contribute to a general knowledge of such structures.

When the waves cross the breakwater, the process of wave breaking and the nonlinear interaction process between the components of the wave spectrum occur. Nonlinear interactions between wave components cause a transfer of wave energy from primary harmonics to higher harmonics of the wave spectrum. The amount of energy transferred depends on the incoming wave parameters, breakwater geometry and water depth. Beji and Battjes (1993) observed wave energy amplifications at high frequencies as waves propagate over a submerged bar in a laboratory experiment. They found that bound harmonics are amplified during the shoaling process and released in the deeper water region after the bar crest. In the process of transition across the breakwater the nonlinear behaviour of waves and a deviation from Gaussian as well as Rayleigh distribution occur. Zou and Peng (2011) found that wave skewness as a primary wave nonlinearity indicator varies across a submerged bar. Their results show that wave skewness decreases slightly above the seaward slope, increases rapidly up to a maximum value above the structure crest, and then decreases above the leeward slope to the value close to incident. Based on the measurements of the surface elevations in the wave channel, this paper proves that, at a certain distance from the breakwater, transmitted surface elevations have Gaussian distribution and wave heights behave according to Rayleigh's distribution (Sections 2 and 3).

The general conclusion of the works of Goda et al. (1974), Tanimoto et al. (1987), Raichlen et al. (1992) is that when the waves cross the breakwater with a low positioned crown, mean spectral wave periods are reduced by 60% in relation to the incoming mean wave periods. Goda et al. (1974) found for emerged breakwater that reduction of mean wave periods depends on relative submergence R_c/H_{m0} and zero freeboard periods are reduced by approximately 30%. The general conclusion is that the transfer of energy to higher harmonics of the wave spectrum causes a transformation of zero crossing and spectral wave periods. Therefore, this study will deal with the impact of breakwater submergence and incident wave parameters on the transformation of wave periods (Section 4).

Hamm and Peronnard (1997) have investigated the influence of high-frequency turbulent fluctuations and low-frequency waves on the accuracy of temporal analysis. They concluded that high-frequency waves could significantly harm the calculation of periods in the nearshore area. Using the same algorithm as Hamm and Peronnard (1997), this work investigates the influence of the short and long waves

* Corresponding author. Tel.: +385 915008005; fax: +385 14639238.
E-mail addresses: car@grad.hr (D. Carevic), goran.loncar@grad.hr (G. Loncar), mprsic@grad.hr (M. Prsic).
[1] Tel.: +385 14864 448; fax: +385 14864 450.
[2] Tel.: +385 14639611; fax: +385 14639238.

0378-3839/$ – see front matter © 2013 Elsevier B.V. All rights reserved.
http://dx.doi.org/10.1016/j.coastaleng.2013.04.004

generated when waves cross the submerged bar on the temporal analysis (Section 4).

Van der Meer et al. (2000), conducted tests on emerged smooth breakwaters and reached the conclusion that mean spectral wave period is reduced by up to 40% in relation to the incoming mean wave period. Based on measurements, they developed a very crude model for calculating transmitted energy spectra, where they proposed that 40% of spectrum energy is positioned at frequencies between $1.5f_p$ and $3.5f_p$, and 60% of energy at $f < 1.5f_p$. Van der Meer et al. (2005) confirmed that model experimentally on emerged and submerged structures. The main weakness of this model is that energy transfer to higher harmonics is independent of incident wave parameters or construction geometry. In this work the improvement of the Van der Meer et al. (2000) model was made based on the conclusion that the energy fraction transferred to high frequencies is variable with submergence and reaches the published value 40% (Van der Meer et al., 2000, 2005) when the breakwater crest is around water level. Based on a linear approximation of the value of this fraction and on the assumption that energy is uniformly transferred to the frequency range ($1.5f_p$–$3.2f_p$) a satisfactory description of the mean period reduction over smooth impermeable breakwater is obtained (Section 5). The paper by Briganti et al. (2003) studies the impact of transmission coefficients of wave height on the transfer of energy from lower to higher harmonics. They introduced a parameter named energy density parameter (e.d.p.), which describes how much energy is transferred to higher frequencies in the process of wave transmission. In this work the e.d.p. was used to detect the submergence at which the transition of energy to higher frequencies starts/ends (Section 5).

By developing an analytical calculation model, the process of wave transmission and spectral change over a permeable low-crested breakwater is described in the papers of Lamberti et al. (2007) and Zanuttigh and Martinelli (2008). In these works the authors developed an analytical model for emerged low-crested breakwaters able to predict transmitted wave spectrum based only on incident wave conditions and structure geometry. The proposed model is based on a combination of wave transmission through (filtration) and over the structure (overtopping).

This paper represents an extension of an endeavor to develop relatively simple analytical models for the calculation of transmitted spectra. The subject is on (very) large wave transmission, which is an extension of earlier works with emerged and zero freeboard structures.

The objectives of the paper are the following: (1) to show that away from the breakwater, waves behave as a Gaussian process and according to Rayleigh's distribution (independent propagation of components, Sections 2 and 3), (2) to quantify the effect of superharmonics generation, i.e. spectral broadening and mean period reduction (Section 4) and (3) to improve the analytical Van der Meer et al. (2000) model in the area of large wave transmission coefficients (submerged breakwater).

2. Laboratory measurements

Laboratory tests were conducted by piston wave generator using the active wave absorption control system (AWACS). At the end of the channel was the dissipation chamber which gives a maximum reflection coefficient of 0.2 for the longest wavelengths from Table 1. The wave channel width was 1 m, the height was 1.1 m, and the depth of water in the channel was $d_1 = 0.4$ m and $d_2 = 0.446$ m. The submerged breakwater model was made of wood, the crest width being $B = 0.16$ m and the slope 1:2 (Fig. 1). The measurements were performed for two submersions of the wave crown ($R_{c1} = 0.055$ m and $R_{c2} = 0.101$ m) achieved by changing the depth of the water in the channel ($d_1 = 0.4$ m and $d_2 = 0.446$ m). Measurements were performed in conformity with Table 1 for each depth, totaling in 18 measurements. Time duration for an experiment amounts to ~5 min, which is approx. 300 waves per experiment, pursuant to the recommendations from Journée and Massie (2001). The acquisition of the data was performed with a sampling frequency of 40 Hz.

2.1. Data processing

Capacitive gauges G1–G6 were used for measuring surface elevation. The measured data were processed according to two methods: spectral (frequency domain) and zero-crossing (time domain).

According to the spectral principle, spectral wave parameters were established as: H_{m0}, $T_{0,2}$ and T_p (defined in the list of symbols at the end). The incident wave parameters were determined by separating the incoming and the reflected spectrum on the gauges G1–G3, and transmitted wave parameters by separation on the G4–G6 gauges. The Zelt and Skjelbreia (1992) method was used for separating the incident from the reflected spectrum.

The zero-crossing wave parameters H_{max}, $H_{1/10}$, $H_{1/3}$, H_m, H_{rms}, $T_{1/3}$ and T_z have been defined by up-zero crossing method for incident and transmitted surface elevation time series, determined by two approaches:

(a) inverting the FFT of the incident and the transmitted spectrum defined by procedure described in the previous paragraph;
(b) wave record from gauge G1 was assumed to be an incident wave and wave record from G4 a transmitted one. This approach is used to extract Figs. 2b, 7 and 8.

In the temporal domain, surface elevation time series were then processed to remove low-frequency waves using a high-pass filter with a cut-off frequency equal to half the peak incident wave frequency. The next step was the removal of high-frequency waves from the same time series using a low-pass filter with cut-off frequencies of $3.5f_p$ and $1.5f_p$. This way time series for approaches (a) and (b) were obtained and both include: (1) time series without any filtering (no filt),

Table 1
Wave parameters measured in laboratory obtained from Zelt and Skjelbreia's (1992) separation method, the target was the standard JONSWAP spectrum ($g = 3.3$, $s_1 = 0.07$, $s_2 = 0.09$).

$R_{c1} = -0.055$ m							$R_{c2} = -0.10$ m						
Test	Measured incident			Measured transmitted			Test	Measured incident			Measured transmitted		
	H_{m0-i} [m]	$T_{0,2-i}$ [s]	T_{p-i} [s]	H_{m0-t} [m]	$T_{0,2-t}$ [s]	T_{p-t} [s]		H_{m0-i} [m]	$T_{0,2-i}$ [s]	T_{p-i} [s]	H_{m0-t} [m]	$T_{0,2-t}$ [s]	T_{p-t} [s]
1.	0.060	0.66	0.68	0.040	0.65	0.80	10.	0.062	0.66	0.69	0.053	0.69	0.80
2.	0.058	0.72	0.81	0.041	0.65	0.80	11.	0.065	0.72	0.81	0.055	0.72	0.85
3.	0.055	0.85	1.01	0.041	0.69	0.98	12.	0.064	0.85	1.01	0.057	0.80	0.98
4.	0.099	0.81	0.89	0.051	0.73	0.91	13.	0.103	0.81	0.89	0.076	0.80	0.98
5.	0.096	0.92	1.10	0.055	0.77	1.07	14.	0.105	0.92	1.10	0.081	0.85	1.07
6.	0.089	1.15	1.45	0.058	0.85	1.42	15.	0.106	1.15	1.45	0.084	0.93	1.42
7.	0.121	0.89	0.99	0.058	0.79	0.98	16.	0.126	0.89	0.99	0.087	0.85	0.98
8.	0.113	1.01	1.24	0.062	0.82	1.16	17.	0.127	1.01	1.24	0.091	0.89	1.28
9.	0.104	1.32	1.68	0.066	0.95	1.71	18.	0.126	1.32	1.68	0.094	1.01	1.71

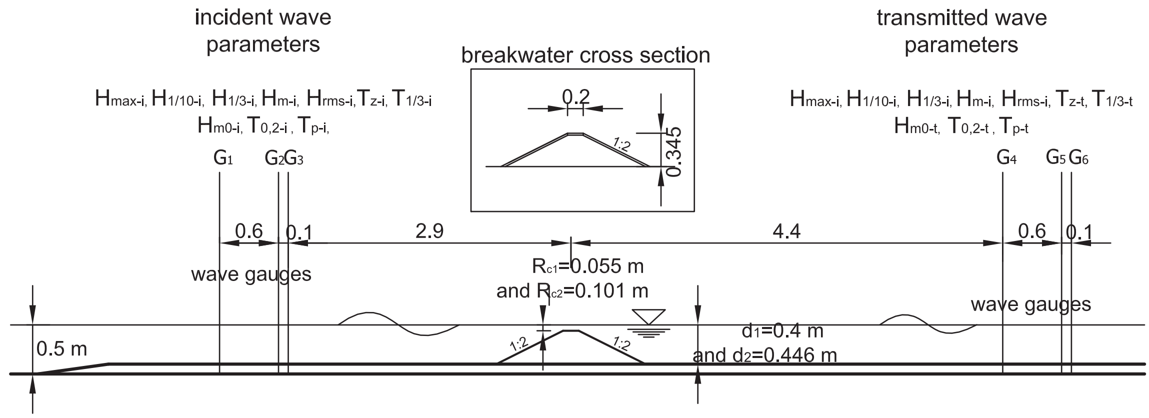

Fig. 1. Details of the wave flume and measured incident and transmitted wave parameters (see list of symbols at the end).

(2) low-frequency wave removal (filt <0.5f_p), (3) high-frequency wave removal (filt <0.5f_p, >3.5f_p) and (4) linearized time series (filt <0.5f_p, >1.5f_p). The Lanczos filter was used for data filtering as described by Godin (1972) in his tide measurement analysis manual (also in Hamm and Peronnard, 1997).

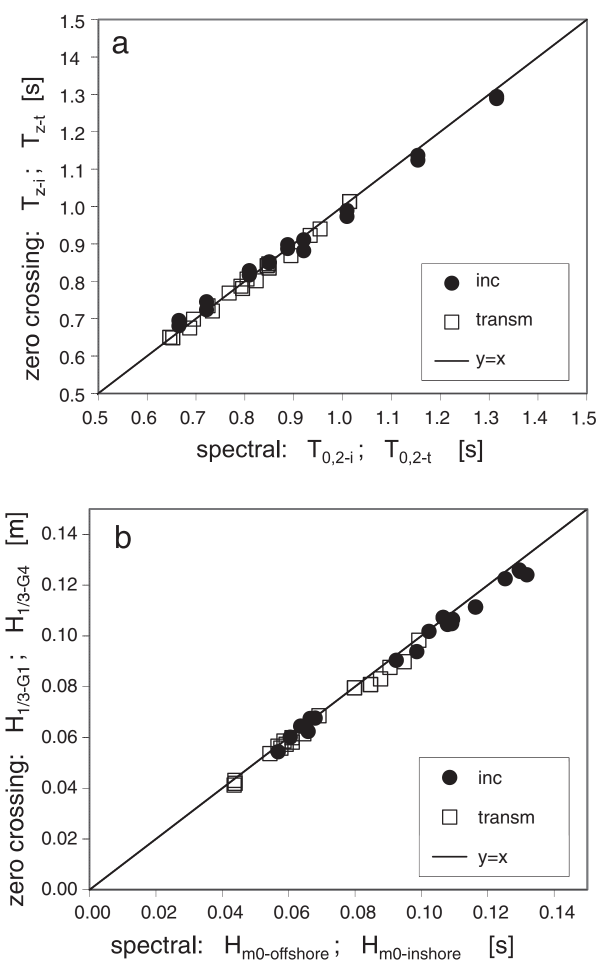

Fig. 2. (a) Ratio of spectral and zero-crossing wave periods, T_z and $T_{0,2}$, for incident and transmitted waves where T_z was defined from zero-crossing method approach (a) and $T_{0,2}$ by Zelt and Skjelbreia's (1992) method. (b) Ratio of measured zero-crossing significant wave heights on gauges G1 ($H_{1/3\text{-}G1}$) and G4 ($H_{1/3\text{-}G4}$) with significant wave heights calculated as the synthesis of incident and reflected spectra at gauges G1 + G2 + G3 ($H_{m0\text{-}offshore}$) and at G4 + G5 + G6 ($H_{m0\text{-}inshore}$) as defined by Zelt and Skjelbreia's (1992) method.

The wave flume is the region divided by the submerged breakwater into two parts. In the immediate vicinity in front of the structure the fixed phase relation between incident and reflected waves causes a spatial variation of zero-crossing parameters (Goda, 2000). To avoid this phenomenon the positions of gauges were chosen to be a minimum of one wavelength offshore from the structure, as proposed by Goda (2000). Nonlinear behaviour at the breakwater causes phases of the fundamental and the superharmonics to be locked at the breakwater, and a sufficient distance is necessary to let the phase change due to the dispersive character of the waves (to behave as a Gaussian process). So, it is important that the distance of inshore gauges is sufficient to avoid nonlinearities and to secure reliable wave analysis. The reliability of the wave analysis is checked verifying that:

1. The elevation distribution is symmetric (Gaussian process). Skewness is the parameter which indicates asymmetry and wave nonlinearity so this parameter was calculated for each gauge from G1 to G6, where low frequencies from raw wave record were removed below half f_p. The calculated skewness ranged from 0.22 to 0.52 for incident waves and from 0.1 to 0.32 for transmitted waves, which indicates that waves are weakly nonlinear. These values are in good agreement with the results of Zou and Peng, 2011, who investigated numerically and experimentally the evolution of skewness across a low crested structure.
2. The wave height is Rayleigh distributed which is shown in Section 3.
3. The mean zero-crossing period T_z is equal to spectral $T_{0,2}$. Fig. 2a presents the relationship between zero-crossing and spectral wave periods for incident and transmitted waves. In the case of incident waves, a comparison of mean spectral $T_{0,2-i}$ and mean zero crossing T_{z-i}, is shown, while for transmitted waves, $T_{0,2-t}$ and T_{z-t} were compared. Spectral periods were derived from Zelt and Skjelbreia's (1992) method and zero crossing was calculated based on the data from approach (a). Good agreement confirms the theoretical result that for a Gaussian process T_z is equal to the period $T_{0,2}$, i.e. it confirms the assumption of independent propagation of components and linear wave propagation at the position of the wave gauges.
4. The zero-crossing wave heights ($H_{1/3\text{-}G1}$, $H_{1/3\text{-}G4}$) are equal to wave heights calculated as a synthesis of incident and reflected components derived from Zelt and Skjelbreia (1992) ($H_{m0\text{-}offshore}$, $H_{m0\text{-}inshore}$). In the case of incident waves, a comparison of $H_{1/3\text{-}G1}$ and $H_{m0\text{-}offshore}$ is shown, while for transmitted waves, $H_{1/3\text{-}G4}$ and $H_{m0\text{-}inshore}$ were compared. Zero crossing wave heights were obtained from records measured at gauges G1 and G4 (approach (b)) and spectral wave heights were obtained as synthesis of incident and reflected components derived from Zelt and Skjelbreia (1992), separately for offshore gauges (G1 + G2 + G3) and for inshore gauges (G4 + G5 + G6) (Fig. 2b).

5. Wave statistics are independent from the position of the wave gauge. Standard deviations of significant wave heights and periods were calculated for records from each group of gauges, offshore (G1–G3) and inshore (G4–G5). It was found that the maximum standard deviation that occurs is 0.0037 for which the difference between maximum and minimum $H_{1/3}$ is 7%. The same procedure was done with significant wave periods where the maximum standard deviation is 0.0572 which corresponds to the maximum difference between significant wave periods of also 7%. All other differences are smaller so it could be concluded that wave statistics are not influenced by the position of the wave gauge.

These findings prove that waves behave, with good approximation, as a Gaussian process at the positions of gauges which secures a reliable wave analysis, conducted further in this paper.

3. Influence of wave transmission on wave height Rayleigh's distribution

If the range of frequencies in a wave record is such that it is a narrow-banded frequency spectrum and the water surface elevation is a Gaussian distribution then the wave height statistics will obey Rayleigh's distribution. Depending on wave height distribution from a wave record, the interrelation of zero crossing wave heights: H_{max}, $H_{1/10}$, $H_{1/3}$, H_m, and H_{rms} and spectral moment m_0 could be defined (Fig. 3). An estimate of these values is made from the time series after the breakwater for approach (a) and for low-frequency wave removal ('filt $<0.5f_p$'). Straight lines corresponding to the theoretical Rayleigh's distribution are also shown. The theoretical relation $H_{max} = 6.762(m_0)^{0.5}$ was estimated on the basis of 300 waves in average time series, corresponding to Rayleigh's distribution.

It may be seen in Fig. 3 that the characteristic wave heights after the breakwater behave according to Rayleigh's distribution. Values are slightly lower (~5%) than the theoretical values, for all representative heights except for H_{max}. This underestimation is characteristic of all values (and also for incident waves, which is not shown herein), so it was assumed that the main reason for this is numerical error in the calculation of inverted FFT. After the breakwater, Rayleigh's distribution is preserved because of the deshoaling process on the shoreward side of the bar. Namely, at the seaward side and crest of the bar partial nonlinear interactions and wave breaking occur, which include the increase of the vertical asymmetry of the incident wave

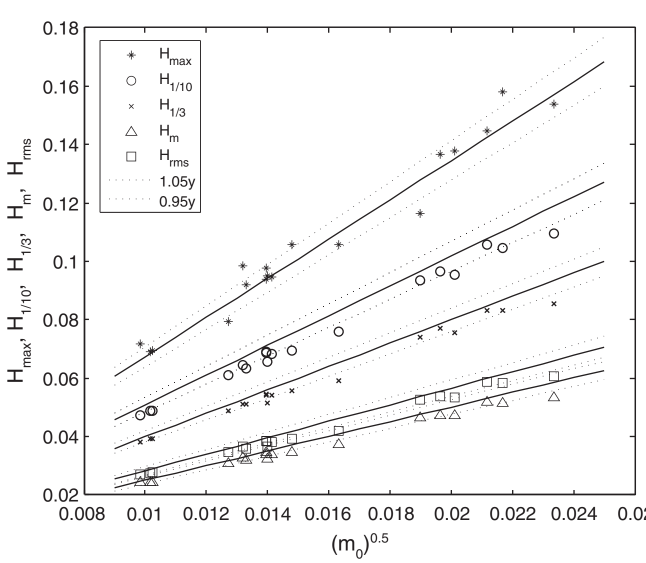

Fig. 3. Relations of zero-crossing wave heights measured after the breakwater compared with theoretical Rayleigh's relations (straight lines) for approach (a) and for low-frequency wave removal ('filt $<0.5f_p$').

profile (increasing skewness and kurtosis, Zou and Peng (2011)) and the occurrence of free tail waves (Beji and Battjes, 1993). In such conditions the distribution of wave heights is very similar to that in shallow water at a sloped beach, where wave heights deviate from Rayleigh's distribution (Battjes and Groenendijk, 2000; Glukovskiy, 1966). At the shoreward side of the bar, the deshoaling process includes the transfer of energy from primary waves to their harmonics and the linearization of the wave profile with the redistribution of wave heights according to Rayleigh's distribution. The examples of Raleigh's probability distributions for Tests 4 and 16 are presented in Figs. 4 and 5, respectively.

Fig. 6 shows a comparison of wave height transmission coefficient K_t defined from the measurements in this paper and the measurements in the paper of Van der Meer et al. (2000) with theoretical coefficients defined by Van der Meer et al.'s (2003) formula (Eq. (1)). It can be seen from this figure that this work deals with large transmission (large submersion), and in that sense this work provides an extension of the previous works for emerged smooth breakwaters (Van der Meer et al., 2000).

4. Reduction of wave periods due to wave transmission over the breakwater

The process of non-linear interaction can be explained in view of physics in the following way: when a longer wave from the irregular wave train crosses the breakwater, generation of bound superharmonics occurs, so that wave train zero-crossing periods are reduced. It can be seen in Fig. 7 that the transmitted wave record ('G4-no filt') is harmed by low-frequency waves which cause a greater number of transmitted waves compared to 'G1-no filt'. For example, from the 1200th to the 1400th time step, a transformation from four to five waves (calculated by zero-up crossing method) is evident. When low and high-frequency waves were filtered from the record, the time series shown on the lower graphs were obtained. From graph 'G4-filt $<0.5f_p$, $>3.5f_p$' it is obvious that a part of the high-frequency waves is removed and the graph 'G4-filt $<0.5f_p$, $>1.5f_p$' shows a totally linearized time series. The same is observed for the filtering process on the incident wave signal but with a lower intensity because of a smaller part of high frequencies.

The generation of superharmonics is evident in waves of considerable length, while it is less noticeable in shorter waves. Fig. 8 presents the influence of relative submergences R_c/H_{m0-i} and wave steepness s_{op} on the amplification of the transmitted number of waves $NW_{trans}^{no\ filt}$ in relation to $NW_{inc}^{no\ filt}$, for waves from Table 1. The number of incident and transmitted waves has been defined from the wave records at gauges G1 and G4 according to approach (b) because only this approach saves the original number of waves. Fig. 8 shows that the number of transmitted waves increases when submergence R_c/H_{m0-i} tends to zero. In the case of the longest waves (low steepness, $s_o = 0.028$–0.041) the number of transmitted waves increases up to 40% of the incident number of waves. Generally, smaller waves are less influenced because nonlinear interactions are less intensive in the shoaling process (on seaward side and crest of the bar). In other words, depth to wave length and depth to wave height ratios are larger.

The same figure presents the influence of signal filtering on the transmitted number of waves NW_{trans}. Points for 'filt $<0.5f_p$' are somewhat higher than points for 'no filt' because when low-frequency waves are removed from the wave record, the wave troughs and crests located a short distance from the mean wave level fall on another side of the mean level and cause new zero-crossing and consequently a larger number of waves (see for example Fig. 7, G4-filt $<0.5f_p$, $>3.5f_p$', near step 800). When high-frequency waves ('filt $<0.5f_p$, $>3.5f_p$') are removed, the number of transmitted waves falls, but the influence is not so significant except for some values of low-stepness waves ($s_{op} = 0.024$–0.04).

Relatively high steepness ($s_{op} = 0.079$–0.083) occurs because the generated incident spectra for tests 1, 4, 7, 10, 13 and 16 slightly

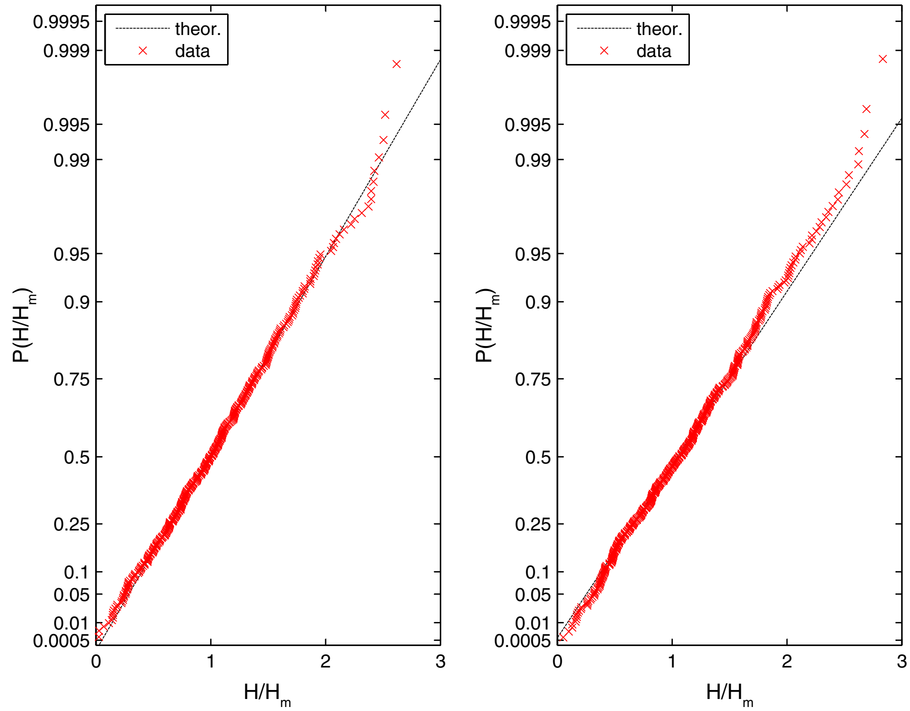

Fig. 4. Rayleigh's distribution of incident (left) and transmitted (right) waves for test 4 (Table 1), for approach (a) and for low-frequency wave removal ('filt <0.5f_p'). Skewness for recorded time series on gauge G1 was S = 0.45 and on G4 S = 0.19.

deviate from the standard JONSWAP spectrum in the area of higher harmonics.

The generated higher harmonics are smaller than for the standard JONSWAP, which causes smaller values of 4th spectral moments (m_4) and consequently smaller intensity of wave breaking which leads to higher values of wave steepness (Massel, 2007).

Mean zero-crossing wave period T_z is directly connected to the number of waves NW. An increase in the number of short waves at the inshore side of the breakwater causes a reduction of the mean zero-crossing periods. The reduction of the transmitted mean zero-crossing wave period T_z in relation to R_c/H_{m0-i} is presented in Fig. 9. Zero-crossing periods (T_z) were defined by inverting the

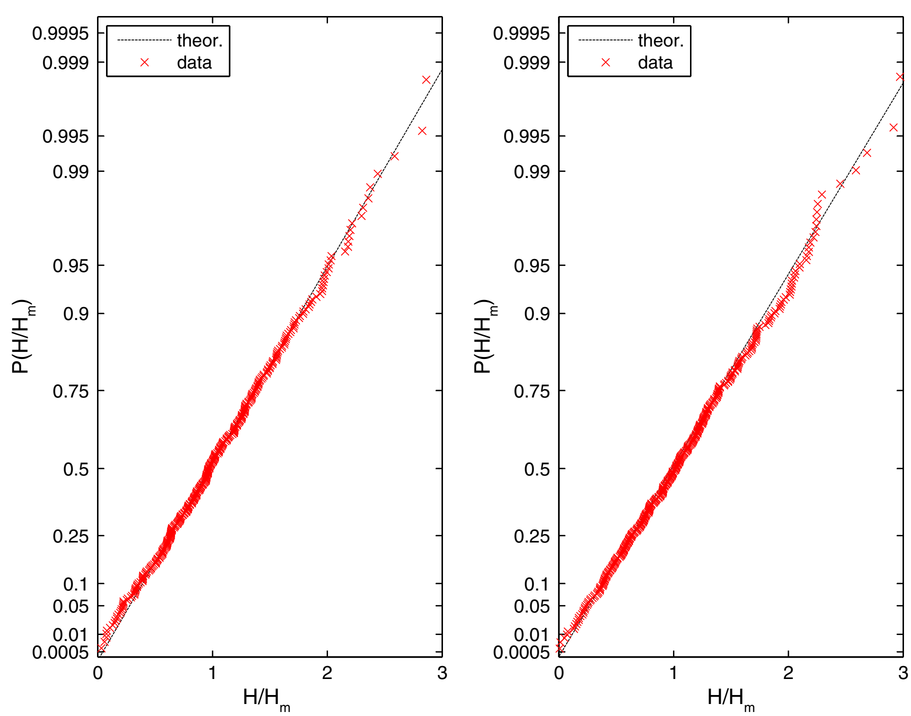

Fig. 5. Rayleigh's distribution of incident (left) and transmitted (right) waves for test 16 (Table 1), for approach (a) and for low-frequency wave removal ('filt <0.5f_p'). Skewness for recorded time series on gauge G1 was S = 0.37 and on G4 S = 0.24.

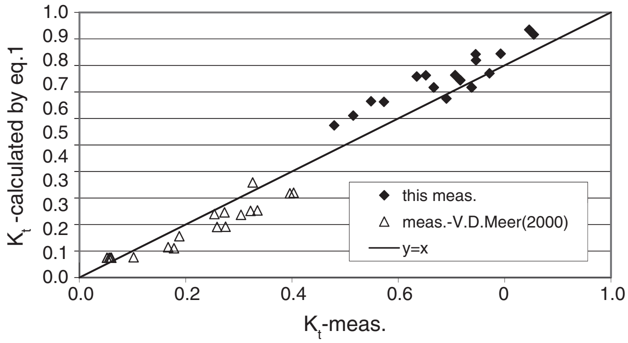

Fig. 6. The comparison of wave height transmission coefficient K_t for measurements in this paper and the paper of Van der Meer et al. (2000) with theoretical values according to Van der Meer et al.'s (2003) formula (Eq. (1)).

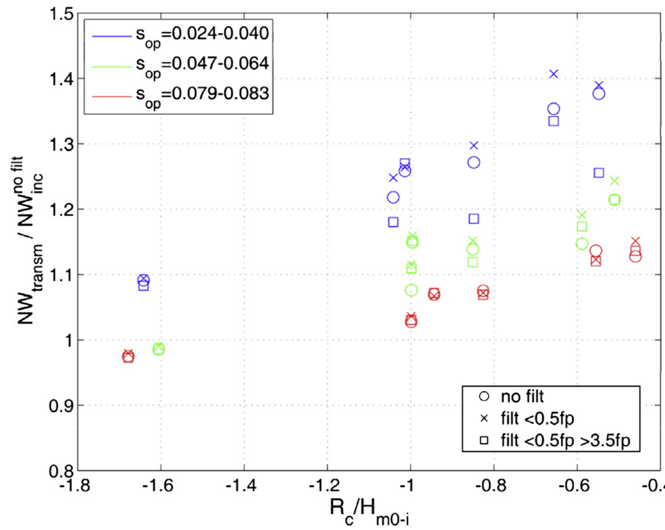

Fig. 8. Ratio of transmitted NW_{trans} and incident NW_{inc} number of waves in relation to relative submergence R_c/H_{m0-i}, for wave records from approach (b) where the incident wave was assumed to be a record from gauge G1 and transmitted from gauge G4.

FFT of the incident and the transmitted spectra according to approach (a). The reduction of the mean period T_z occurs because it covers all waves from the time series, including all newly-formed superharmonics. A strong relationship between relative submergences R_c/H_{m0-i} and period reductions is evident. For smaller waves (lesser $-R_c/H_{m0-i}$ and larger s_{op}) there is small or no reduction of wave periods at all because the transmitted time series is not harmed by newly-formed superharmonics.

The usage of low- and high-frequency filtering ('filt $<0.5f_p$, $>3.5f_p$') does not significantly influence period reduction but the small difference between 'filt $<0.5f_p$' and 'filt $<0.5f_p$, $>3.5f_p$' is noticeable for the low-stepness waves ($s_{op} = 0.024$–0.04). This difference is caused by the removal of the high-frequency waves from frequencies $f > 3.5f_p$. The question which arises here is whether there are waves which have significant energy at frequencies $f > 3.5f_p$ or this part could be removed by filter. To define this, the following calculations were conducted: from the incident and transmitted wave time series (for approach (a)) low-frequency waves were removed ('filt $<0.5f_p$'). Next, zero crossing method was applied to define wave-by-wave parameters, which are sorted in descending order according to periods. Then, calculations of root mean square wave heights of all waves (H_{rms}) and of waves which correspond to frequencies higher than $3.5f_p$ ($H_{rms}^{(high)}$) were conducted. The aim of these calculations was to compare the wave energy on frequencies higher than $3.5f_p$ ($H_{rms}^{2\,(high)}$) to the energy of all waves (H_{rms}^2). The results are shown in Fig. 10. It can be concluded that the energy for frequencies higher than $3.5f_p$ reaches up to 10% of all energy (H_{rms}^2) for the longest waves, which is not insignificant, thus it is questionable to talk about insignificant waves. Filtering at frequencies

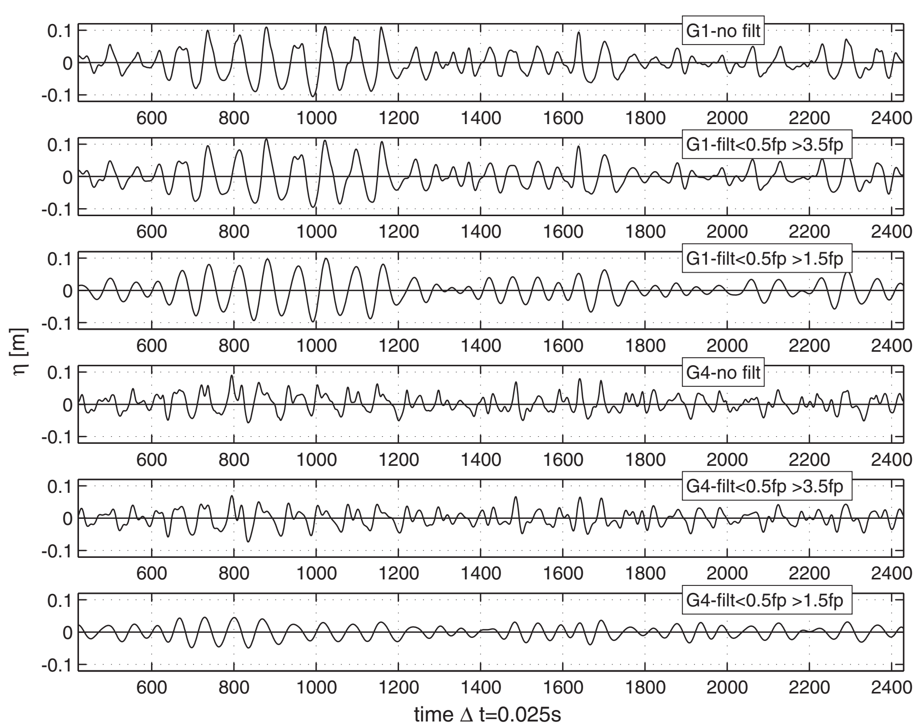

Fig. 7. Incident and transmitted wave time series (no filt, filt $<0.5f_p$, $>3.5f_p$ and filt $<0.5f_p$, $>1.5f_p$) for wave records from approach (b) where the incident signal was assumed to be a signal from gauge G1 and transmitted from gauge G4 (test 18., Table 1). The time series for transmitted wave signal are shifted for 5.2 s to the left at the timescale with the aim of better comparison with the incident wave time series.

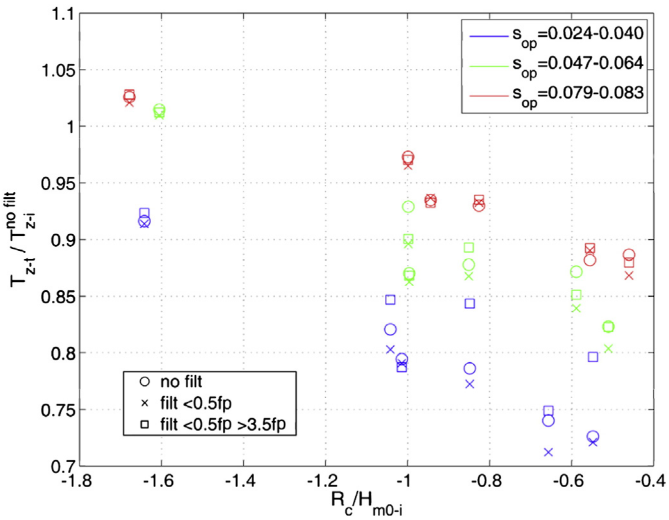

Fig. 9. Reduction of transmitted wave period T_z in relation to the relative submergence R_c/H_{m0-i} for different wave steepness values where the wave time series is defined by inverting the FFT of the incident and transmitted spectra (approach (a)).

$3.5f_p$ or higher is not acceptable because frequencies $>3.5f_p$ carry a certain part of the wave energy so with their removal this part of energy will be lost. The conclusion is that the removal of high- and low-frequency waves from the transmitted wave signal ('filt $<0.5f_p$, $>3.5f_p$') does not influence the temporal analysis of the wave periods and thus it is not recommendable, especially because of certain parts of the wave energy positioned on high frequencies.

It has already been mentioned that in the process of wave transmission over the breakwater, the wave energy is transferred to higher frequencies, along with the increase of the term m_2 (second moment), resulting in the reduction of the mean spectral wave period of transmitted waves $T_{0,2}=\sqrt{m_0/m_2}$ and the reduction of the parameter $T_{0,2-t}/T_{0,2-i}$ in the function of relative submersion R_c/H_{m0-i} (Fig. 11). The data from Van der Meer et al.'s (2000) study for smooth emerged breakwaters with a similar geometry of the breakwater and similar wave parameters as in this paper are used for comparison. In such a way, the presentation of reduction of the mean spectral wave periods $T_{0,2}$ for a wider range of relative submersion is obtained.

It can be seen in the above figure that the ratio $T_{0,2-t}/T_{0,2-i}$, for the range of steepness $s_o=0.024$–0.040, tends to the value of ~0.68 when the relative submersion R_c/H_{m0-i} aims to zero, taking it either from the positive or the negative side. The results of Van der Meer's measurements for the emerged breakwater are closer to this value, since the measurements were made for the lower parameter R_c/H_{m0-i}. Data for the lower and moderate steepness show a similar behaviour for negative submergence except for a zero freeboard intersection which is at the higher level.

5. Spectral change due to wave transmission

The transmitted spectrum is quite different from the incident spectrum. The model for the calculation of spectral change was first given by Van der Meer et al. (2000). This model assumes the distribution of 40% of all transferred energy on higher frequencies (between $1.5f_p$ and $3.5f_p$) and 60% on lower frequencies ($<1.5f_p$). This is a very crude description of spectral deformation and does not include the influence of wave parameters and breakwater submergence. In the work of Van der Meer et al. (2005) this model was experimentally confirmed and much wider ranges of spectral change parameters were given. It was therefore suggested that a part of energy at higher frequencies is between 30 and 60%, and the range of higher frequencies varies between $1.5f_p$ and 2.9–$5.6f_p$.

The above proposed model (with 40%/60% distribution on frequencies $1.5f_p$–$3.5f_p$) was used to calculate the reduction of the mean spectral period ($T_{0,2-t}/T_{0,2-i}$) for a wide range of incident wave parameters: $-1.66\le R_c/H_{m0-i}\le 1.66$. For the calculation of the wave height transmission coefficient, the Van der Meer et al. (2003) formula was used:

$$K_t=\left[-0.3R_c/H_{m0-i}+0.75\left[1-\exp\left(-0.5\xi_{op}\right)\right]\right] \qquad (1)$$

with a minimum of 0.075 and a maximum of 0.8 (see list of symbols at the end). The breakwater slope angle was a = 1:2, and wave steepness $s_{op}=0.02$–0.1. The conclusion was that with this model the ratio $T_{0,2-t}/T_{0,2-i}$ remains the same, regardless of the input wave parameters. The model always gives the same result ($T_{0,2-t}/T_{0,2-i}$) = 0.68. This value is very close to that estimated in Fig. 11, for zero submersion and low steepness $s_o=0.024$–0.040. This is not a coincidence, because the recommendations for this model (energy distribution 40%/60% and $f_{max}/f_p=3.5$) are given as average values for all measurements.

The values of the mean period reduction ($T_{0,2-t}/T_{0,2-i}$) calculated by this model (Van der Meer et al., 2000) depend on the parameter f_{max}/f_p and energy distribution, so the main task of this work is to connect these parameters to incident wave parameters and breakwater submergence.

The submersion of the breakwater crest is the parameter with the greatest influence on spectral change (dissipation of energy and transfer of energy to higher frequencies). If the submerged breakwater is deep enough, spectral change will not arise at all. If the submersion decreases gradually spectral change will be more pronounced. Spectral change consists of the dissipation of energy due to wave breaking and the transfer of energy to higher frequencies. Under the assumption that these two processes are independent, the transfer of energy to higher frequencies is independently related to submersion. It will also be assumed that the leading parameter for the intensity of energy transfer to higher frequencies is R_c/H_{m0-i}, which has a foothold in the interrelation between the mean period reduction and relative submersion in Fig. 9. The first question that arises is where the transfer

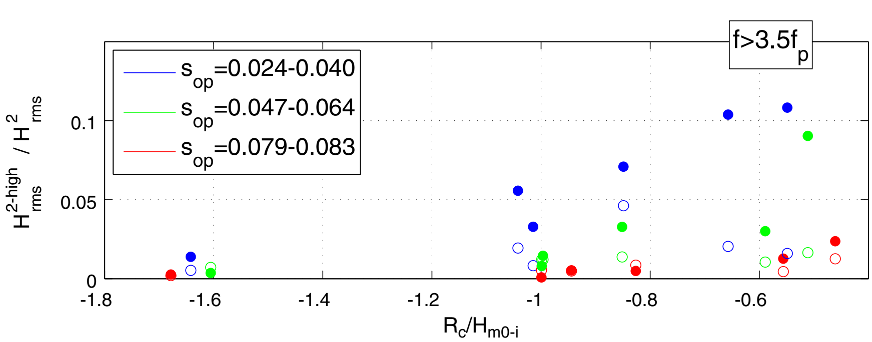

Fig. 10. Comparison of the wave energy on higher frequencies ($f>3.5f_p$) ($H^{2\,(high)}_{rms}$) and the energy of all frequencies (H^2_{rms}) for incident (○) and transmitted waves (●) (for approach (a) and low-frequency removal 'filt $<0.5f_p$').

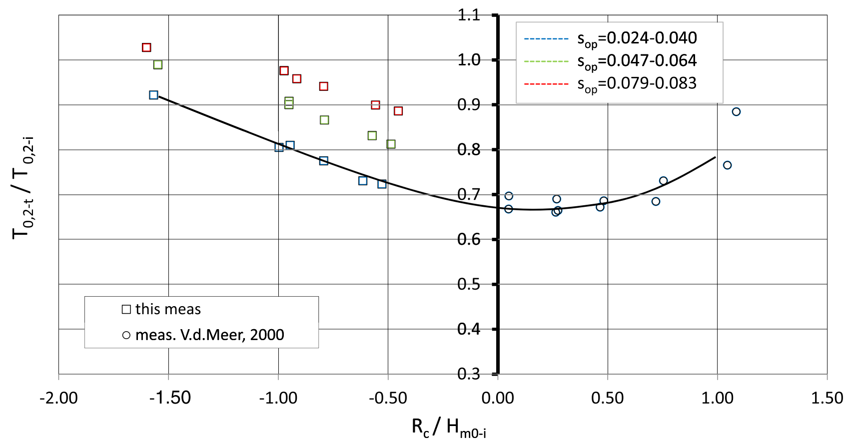

Fig. 11. Dependence of parameter $T_{0,2-t}/T_{0,2-i}$ on relative submersion R_c/H_{m0-i} for smooth breakwater with submerged crown (from this paper) and the emerged crown (as per Van der Meer et al.'s (2000) paper) measurements with crown width $B_b = 0.13$ and 0.3 m; $H_{m0} = 0.09$–0.14 m, wave steepness $s_{op} = 0.027$–0.031, water depth $d = 0.29$–0.37 m, breakwater slope 1:4, $R_c/H_{m0} = 0$–1.0. (For interpretation of the references to color in this figure, the reader is referred to the web version of this article.)

of energy to higher frequencies starts. In that sense the parameter defined by Briganti et al. (2003) named energy distribution parameter (e.d.p.) was used:

$$\text{e.d.p.} = \left[\left(\frac{E_{t1.5}}{E_t}\right) - \left(\frac{E_{i1.5}}{E_i}\right)\right] / \left(\frac{E_{i1.5}}{E_i}\right). \tag{2}$$

The e.d.p. describes the variation of the energy associated with $f > 1.5f_p$ between the incident and transmitted spectra. The e.d.p. is positive if the energy is transferred towards $f > 1.5f_p$ and zero if no energy transmission occurs. Fig. 12 shows the relationship of the e.d.p. and parameter R_c/H_{m0-i}. The rounded two dots represent the two smallest waves from the dataset (tests 10 and 11 from Table 1), for submersion $R_{c2} = 0.10$ m. These two values are around zero, so it can be assumed that the energy transfer for these two tests does not arise. This conclusion is important because this way the threshold value of parameter $E_{t1.5}/E_t = 0.071$ (Fig. 13) where transfer of energy starts/ends for all steepness will be calculated. The constant value $E_{t1.5}/E_t = 0.071$ for all types of steepness is an assumption because such a threshold can vary with steepness and here because of the lack of data it cannot be precisely defined.

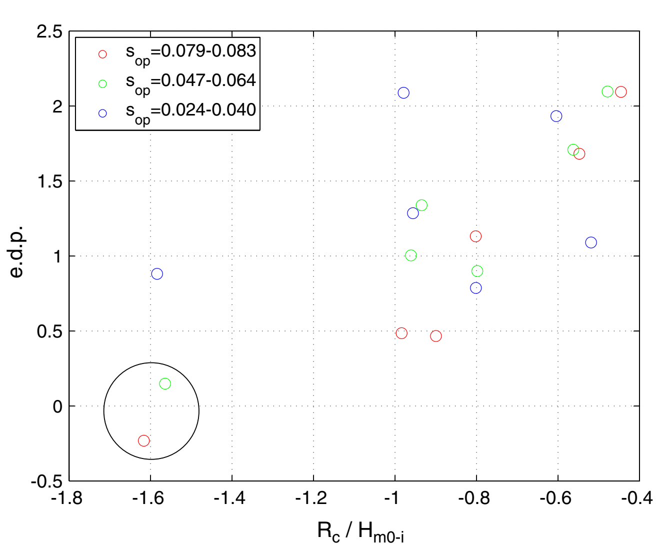

Fig. 12. Correlation of the e.d.p. and R_c/H_{m0-i} for the measured data (Table 1) for approach (a) and low-frequency removal ('filt <0.5f_p'). The rounded values are not influenced by the submerged breakwater.

Fig. 13 presents the correlation of the parameter $E_{t1.5}/E_t$ to the relative submersion R_c/H_{m0-i}. The parameter $E_{t1.5}/E_t$ represents how much energy is positioned on higher frequencies, $f > 1.5f_p$, and according to the Van der Meer et al. (2000) model, it should be around 0.4. From Fig. 13 it is clear that this value varies and is well-correlated to R_c/H_{m0-i} depending on the deepwater wave steepness s_{op}. The linear approximation is used to take this relationship into account. Lines were adjusted to the dots with lower limit at $E_{t1.5}/E_t = 0.071$, which corresponds to the average value of the two lowest positioned dots with the assumption that these two measurements are not influenced by the submerged breakwater (Fig. 12). These two dots correspond to the far left squares in Fig. 11 (red and green), where it can be observed that the reduction of spectral wave periods does not occur. According to the above assumptions the threshold where the transfer of energy starts is $(R_c/H_{m0-i}) \sim -1.9$ for low ($s_{op} = 0.024$–0.040), $(R_c/H_{m0-i}) \sim -1.6$ for moderate steepness ($s_{op} = 0.047$–0.064) and for high steepness ($s_{op} = 0.079$–0.083) is around $(R_c/H_{m0-i}) \sim -1.4$.

The line coefficients in Fig. 13 are linearly approximated in relationship to the wave steepness s_{op}, so the next equation was obtained:

$$\frac{E_{t1.5}}{E_t} = \max\left[0.071,\ \left(-2.71 \cdot s_{op} + 0.32\right)\frac{R_c}{H_{m0}} + \left(-6.21 \cdot s_{op} + 0.71\right)\right]. \tag{3}$$

With the distribution of energy positioned at $f > 1.5f_p$ as represented by Eq. (3), the transmitted mean spectral periods $T_{0,2-t}$ are calculated according to the model of Van der Meer et al. (2000). The results are shown in Fig. 14. Calculations were done for three ranges of deepwater steepness and for parameter $f_{max}/f_p = 3.2$. The line for the improved Van der Meer et al. (2000) model (for low steepness) tends to $T_{0,2-t}/T_{0,2-i} = 0.68$ around zero freeboard which is well-matched with the line for the original Van der Meer et al. (2000) model around zero freeboard. The lines for high and moderate steepness are not in agreement with the original Van der Meer et al. (2000) model because this model is based on measurements with steepness close to the $s_{op} = 0.027$–0.031.

The improved model reaches the value of parameter $(T_{0,2-t}/T_{0,2-i}) = 1$ at different points ($R_c/H_{m0-i} \sim 1.4$, 1.65 and 1.9) depending on the wave steepness, which is in agreement with Fig. 13. The improved Van der Meer et al. (2000) model is sensitive to the ratio f_{max}/f_p. The frequency f_{max} could only be determined by selecting spectrum threshold $S(f_{max})$ from the transmitted spectrum diagram, which introduces uncertainty to this task. Another problem is that f_{max} depends on the incoming wave height, submergence and

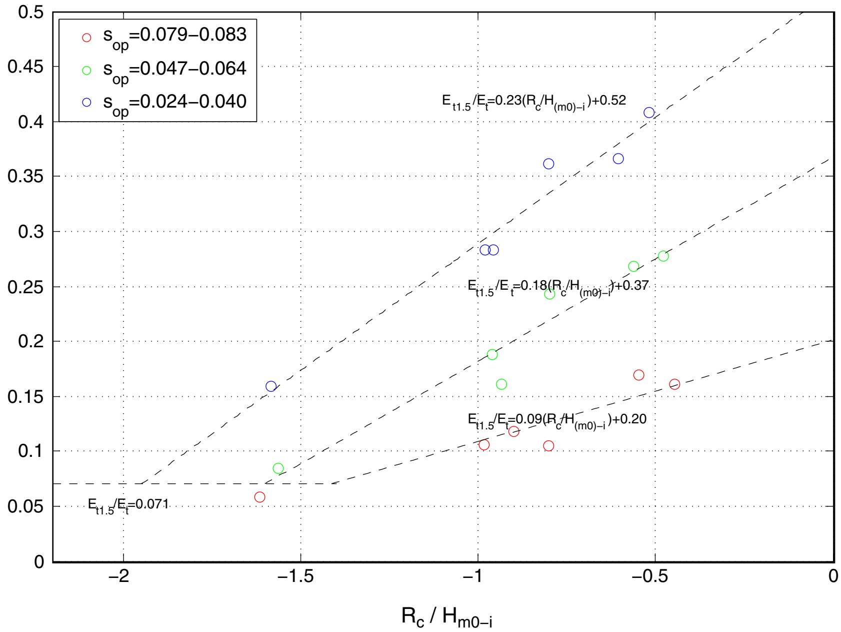

Fig. 13. Correlation of energy on frequencies $f > 1.5f_p$ defined with parameter $E_{t1.5}/E_t$ to the relative submersion R_c/H_{m0-i} for the measured data (Table 1) for approach (a) and low-frequency removal ('filt <0.5f_p').

wavelength, so it gives more complexity to this task. Further research on this topic should be directed towards the functional definition of the ratio f_{max}/f_p.

The use of mean spectral period $T_{0,2} = (m_0/m_2)_{0.5}$, based on the 2nd order spectral moment, could be questionable, because it is very sensitive to high-frequency disturbances. EU Project CLASH suggested to employ either $T_{0,1} = (m_0/m_1)$ or $T_{-1,0} = (m_{-1}/m_0)$ as the most stable index for the period. Therefore the same calculations as those presented previously in the text but with proposed periods $T_{0,1}$ and $T_{-1,0}$ were conducted. The results are very similar to those presented in Fig. 14, so the period $T_{0,2}$ was chosen because of better comparability with zero-crossing periods. Fig. 15 shows examples of the calculated and measured transmitted wave spectra for tests 2 and 14. It is obvious that in the area of high frequencies calculated spectrum is linear approximation of measured spectrum.

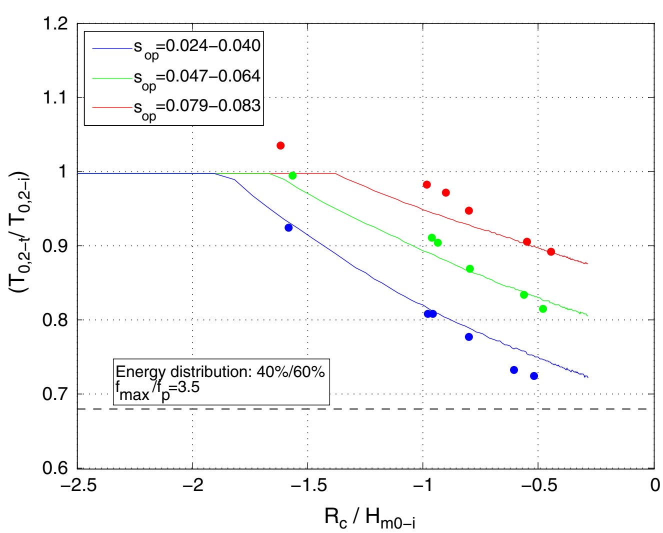

Fig. 14. Reduction of mean period $T_{0,2-t}/T_{0,2-i}$, calculated by the improved Van der Meer et al. (2000) model ("—") and comparison to the original Van der Meer model ("– –") and with measurements ("○") for different deepwater steepness s_{op}.

6. Conclusion

Experimental investigations in the wave channel have been conducted with a smooth submerged breakwater. Tests have shown that when the waves cross the breakwater, in the case of the longest waves, the number of transmitted waves can increase up to 40% of the incident number of waves. Thus, the zero-crossing wave period T_z is reduced. The reduction of wave period depends on the relative submersion, i.e. on the ratio of the breakwater crown submersion and the incoming wave height R_c/H_{m0-i}. The reduction of wave period is more intensive for a smaller submersion, so that the mean wave period T_z, is being reduced by up to 30% in relation to the incoming mean period.

Removal of high- and low-frequency waves from the transmitted wave time series does not influence temporal analysis of wave periods for low-pass removal at $f = 3.5f_p$ and high-pass removal at $f = 0.5f_p$. The wave energy positioned on shorter waves ($f > 3.5f_p$) generated at the rear side of the submerged breakwater can reach up to 10% of the average wave energy of the wave record. Thus, removal of high-frequency waves from the transmitted wave signal is not recommendable, because of the energy positioned on the short waves.

The mean spectral period $T_{0,2}$ depends on the relative submersion R_c/H_{m0-i}, and is reduced as submersion approaches the zero value, for both submerged and emerged breakwaters. It is estimated that the greatest period $T_{0,2}$ reduction when crossing the smooth breakwater occurs when the relative submersion is $R_c/H_{m0-i} \sim 0$ and amounts to ~70% of the value of the incoming mean period.

The empirical model of Van der Meer et al. (2000) for the estimate of the spectral change due to wave transmission has been improved. The assumption of constant distribution of the wave energy on higher harmonics (40%/60%) has been proved to be inadequate, thus the linear distribution of energy in relation to relative submergence was assumed. Under this assumption better agreement between model and measured values was obtained.

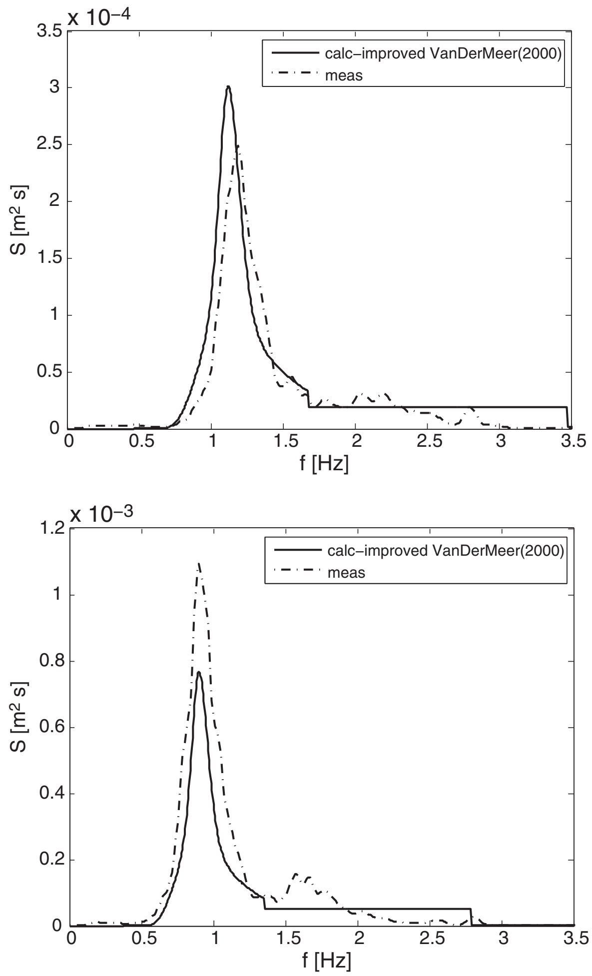

Fig. 15. Examples of the calculated and measured transmitted wave spectra for tests 2 (up) and 14 (down) from Table 1, $f_{max}/f_p = 3.2$.

The representative zero crossing wave heights H_{max}, $H_{1/10}$, H_s, H_{rms} and H_m, after waves crossing the submerged smooth breakwater behave according to the Rayleigh distribution.

List of symbols

ξ_{op}	breaker parameter, $\xi_{op} = \tan\alpha/\sqrt{s_{op}}$
a	breakwater slope angle, [°]
B_b	breakwater crown width, [m]
d	water depth
f_{max}	maximal frequency, $f_p = 1/T_p$, [s]
f_p	peak frequency, $f_p = 1/T_p$, [s]
h	water surface elevation, [m]
H_{m0}	significant wave height, [m], $H_{(m0)} = 4\sqrt{m_0}$
$H_{m0\text{-offshore}}$	significant wave height obtained as synthesis of incident and reflected components derived from Zelt and Skjelbreia (1992) on gauges G1 + G2 + G3, [m], $H_{(m0)} = 4\sqrt{m_0}$
$H_{m0\text{-inshore}}$	significant wave height obtained as synthesis of incident and reflected components derived from Zelt and Skjelbreia (1992) on gauges G4 + G5 + G6, [m], $H_{(m0)} = 4\sqrt{m_0}$
$H_{1/3\text{-G1}}$	significant wave height form record on gauge G1, (zero up-crossing)
$H_{1/3\text{-G4}}$	significant wave height form record on gauge G4, (zero up-crossing)
$H_{1/10}$	1/10th wave height, [m], (zero up-crossing)
$H_{1/3}$	significant wave height, [m], (zero up-crossing)
H_m	mean wave height, [m], (zero up-crossing)
H_{max}	maximum wave height, [m], (zero up-crossing)
H_{rms}	root mean square wave height, [m], (zero up-crossing)
K_t	transmission coefficient of significant wave height, (Eq. (1))
m_0, m_2	zero and second spectral moment, $m_0 = \int_0^\infty S(f)\ df$, $m_2 = \int_0^\infty f^2 \cdot S(f)\ df$
NW	number of waves, calculated by zero-crossing method, (Eq. (1))
$P(H/H_m)$	probability of exceedance of variable H/H_m, (Eq. (1))
R_c	distance from crown to water level, positive if emerged, negative if submerged, [m]
$S(f)$	wave spectra, $[m^2 \cdot s]$
s_{op}	wave steepness, (Eq. (1)), $s_{op} = 2\pi H_{m0}/gT_p^2$
t	time, [s]
$T_{0,2}$	mean wave period, [s], $T_{0,2} = \sqrt{m_0/m_2}$
T_s	significant wave period, [s]
T_z	mean wave period, [s], (zero up-crossing)
T_p	peak wave period, [s]

References

Battjes, J.A., Groenendijk, H.W., 2000. Wave height distributions on shallow foreshores. Journal of Coastal Engineering 40, 161–182.

Beji, S., Battjes, J.A., 1993. Experimental investigation of wave propagation over a bar. Coastal Engineering 19, 151–162.

Briganti, R., Vander Meer, J., Buccino, M., Calabrese, M., 2003. Wave transmission behind low-crested structures. Proceedings of the Coastal Structures.

Glukovskiy, B.Kh., 1966. Investigation of sea wind waves. (In Russian) Leningrad, Gridrometeo-Izdat (reference obtained from E. Bouws. Spectra of extreme wave conditions in the Southern north sea considering the influence of water depth): Proc. Of Sea Climatology Conf., Paris, pp. 51–71.

Goda, Y., 2000. Random seas and design of maritime structures, Second edition. Advanced Series on Ocean Engineering, vol. 15. World Scientific, pp. 356–361.

Goda, Y., Suzuki, Y., Kishira, Y., 1974. Some experiences in laboratory experiments with irregular waves. Proc. 21st Japanese Conf. Coastal Engrg, pp. 237–242.

Godin, G., 1972. The Analysis of Tides. Liverpool University Press.

Hamm, L., Peronnard, C., 1997. Wave parameters in nearshore: a clarification. Coastal Engineering, 32. Elsevier, pp. 119–135.

Journée, J.M.J., Massie, W.W., 2001. Offshore Hydromechanics, First edition. Delft University of Technology 5–43 (http://www.shipmotions.nl).

Lamberti, A., Zanuttigh, B., Martinelli, L., 2007. Overtopping and wave transmission: an interpretation of spectral change at low-crested rubble mound structures. Proc. Coastal Eng. 2006, vol. 5. World Scientific Publishing Co., San Diego, pp. 4628–4640.

Massel, S.R., 2007. Ocean Waves Breaking and Marine Aerosol Fluxes. Atmospheric and Oceanographic Sciences Library, Springer, pp. 91–97. 147, 179.

Raichlen, F., Cox, J.C., Ramsden, J.D., 1992. Inner harbor wave conditions due to breakwater overtopping. Proc. Asce, Coastal Engineering Practice, Long Beach, California, USA.

Tanimoto, K., Takahashi, S., Kimura, K., 1987. Structures and hydraulic characteristics of breakwaters—the states of the art of breakwater design in Japan. Report of the Port and Harbour Research Institute, vol. 26, No. 5.

Van der Meer, J., Regeling, H.J., de Waal, J.P., 2000. Wave transmission: spectral changes and its effect on run-up and overtopping. ASCE, Proc. ICCE, Sydney, Australia, pp. 2156–2168.

Van der Meer, J., Wang, B., Wolters, A., Zanuttigh, B., Kramer, M., 2003. Oblique wave transmission over low-crested structures. ASCE, Proc. Coastal Structures, Portland, Oregon.

Van der Meer, J., Briganti, R., Zanuttigh, B., Baoxing, W., 2005. Wave transmission and reflection at low-crested structures: design formulae, oblique wave attack and spectral change. Coastal Engineering 52, 915–929.

Zanuttigh, B., Martinelli, L., 2008. Transmission of wave energy at permeable low crested structures. Coastal Engineering 55, 1135–1147.

Zelt, J.A., Skjelbreia, J.E., 1992. Estimating incident and reflected wave fields using an arbitrary number of wave gauges. Proceedings of 23rd International Conference on Coastal Engineering, ASCE, pp. 466–480.

Zou, Q., Peng, Z., 2011. Evolution of wave shape over a low-crested structure. Coastal Engineering 58, 478–488.